Kinetic Effects of Myosin Regulatory Light Chain Phosphorylation on Skeletal Muscle Contraction

Julien S. Davis, Colleen L. Satorius, and Neal D. Epstein
Molecular Physiology Section, Laboratory of Molecular Cardiology, National Heart Lung and Blood Institute, National Institutes of Health, Bethesda, Maryland 20892-1760 USA

ABSTRACT Kinetic analysis of contracting fast and slow rabbit muscle fibers in the presence of the tension inhibitor 2,3-butanedione monoxime suggests that regulatory light chain (RLC) phosphorylation up-regulates the flux of weakly attached cross-bridges entering the contractile cycle by increasing the actin-catalyzed release of phosphate from myosin. This step appears to be separate from earlier Ca^{2+} regulated steps. Small step-stretches of single skinned fibers were used to study the effect of phosphorylation on fiber mechanics. Subdivision of the resultant tension transients into the Huxley-Simmons phases 1, 2_{fast}, 2_{slow}, 3, and 4 reveals that phosphorylation reduces the normalized amplitude of the delayed rise in tension (stretch activation response) by decreasing the amplitudes of phase 3 and, to a lesser extent, phase 2_{slow}. In slow fibers, the RLC P1 isoform phosphorylates at least 4-fold faster than the P2 isoform, complicating the role of RLC phosphorylation in heart and slow muscle. We discuss the functional relevance of the regulation of stretch activation by RLC phosphorylation for cardiac and other oscillating muscles and speculate how the interaction of the two heads of myosin could account for the inverse effect of Ca^{2+} levels on isometric tension and rate of force redevelopment (k_{TR}).

INTRODUCTION

The dumbbell-shaped regulatory light chain (RLC) of myosin wraps around and stabilizes a segment of the myosin heavy chain α-helix between the essential light chain and the junction with the myosin rod of the thick filament backbone. In rabbit psoas type IIb fast fibers there is a single RLC species, while there are two different species in rabbit soleus type I slow fibers. Each has a serine that can be phosphorylated by myosin light chain kinase (MLCK) and dephosphorylated by a phosphatase (type I_M). The N-terminal residues 1–18, including the phosphorylatable serine, appear disordered in x-ray structures of the S-1 head of myosin indicating mobility of the segment (Rayment et al., 1993). However, in the complete molecule this segment can interact with the S-1—S-2 hinge region and the proximal part of the S-2 portion of the myosin rod (Xie et al., 1994). Myosin cross-bridges are normally organized as an ordered array on the thick filament surface; upon RLC phosphorylation they release from the surface of the thick filament backbone (Levine et al., 1996). Probe studies reveal that the catalytic and regulatory domains are in fact mobile in the ordered state, but undergo a further 2-fold increase in mobility on phosphorylation (Adhikari et al., 1999). Although simple charge repulsion between the negatively charged backbone of the thick filament and the phosphorylated serine seems plausible, the mechanism appears to be more complex as reviewed by Trybus (1994).

Submitted August 28, 2001, and accepted for publication April 25, 2002.

Address reprint requests to Julien S. Davis, Molecular Physiology Section, Laboratory of Molecular Cardiology, NHLBI, National Institutes of Health, 10 Center Drive, MSC. 1760, Building 10, Room 8N202, Bethesda, MD 20892-1760. Tel.: 301-435-5285; Fax: 301-402-1583; E-mail: davisjs@nhlbi.nih.gov.

0006-3495/02/07/359/12 $2.00

In smooth muscle and non-muscle myosins, phosphorylation of the RLC controls the activation of the myosin ATPase (Trybus, 1994). In striated skeletal/cardiac muscle, however, the main effect of RLC phosphorylation is to increase calcium sensitivity at less than maximal levels of activation with no detectable effect on maximally Ca^{2+}-activated fibers (Persechini and Stull, 1984; Sweeney et al., 1993). The net consequence is that the force-pCa curve is offset to the left, representing higher Ca^{2+} sensitivities with RLC phosphorylation. In pre-steady-state kinetic experiments on skinned fibers it has been shown that the rate of force redevelopment from zero tension increases upon phosphorylation (Metzger et al., 1989; Sweeney and Stull, 1990; Sweeney et al., 1993). A simple "black box" model (Huxley, 1957) in which the rate of formation of the force-generating state(s) (f_{app}) increases on phosphorylation while the rate of decay of the force-generating state(s) (g_{app}) remains unchanged is consistent with various experimental observations. These include parallel increases in isometric fiber tension, stiffness, and ATPase activity and the observation that the offset of the pCa tension curve is greatest at low levels of activation while the offset of the pCa force-redevelopment (k_{TR}) curve is greatest at high levels of activation. Further interpretation of the pre-steady-state mechanisms of this type in muscle fibers is difficult. Analysis requires the application of an array of rapid-reaction analytical and experimental techniques to individually probe each of the series of intermediate states that sequentially form and decay in time during the approach to the isometric steady state (Gutfreund, 1995).

Studies on the in vivo consequences of RLC phosphorylation mostly rely on repetitive electrical stimulation of the muscle to elevate fiber Ca^{2+} levels that in turn activate the Ca^{2+}/calmodulin-dependent MLCK complex to cause an increase in RLC phosphorylation. Repetitive stimulation of

a muscle was found to correlate with increased force per twitch, a phenomenon known as the potentiation of isometric twitch tension (Manning and Stull, 1982; Moore et al., 1985). In yet more elaborate experiments, it appears that RLC phosphorylation correlates with increased work during large 10% sinusoidal changes in muscle length (Grange et al., 1993).

Of all the available perturbation methods (temperature-jump, pressure-jump, ATPase substrate and product concentration-jump and length-jump (L-jump)), the classical Huxley-Simmons (H-S) L-jump (step-stretch/release experiments) is probably the best suited to a study of changes wrought by RLC phosphorylation on the mechanics, and in particular the kinetics, of muscle contraction (Davis, 2000). This is because the step-movement of thick and thin filaments relative to one another elicits responses from all of the attached and transiently attached cross-bridges in the fiber. Our current understanding of the origin and function of the various L-jump phases and their relationship to the cross-bridge cycle is summarized here to provide an interpretative framework for the experimental data. A rapid step-stretch applied to an isometrically contracting fiber causes a "tension transient" during which the tension increase caused by the change in fiber length decays back to the pre-jump isometric tension. Subdivision of the resultant L-jump tension transients into the H-S kinetic phases 1 (amplitude only), 2_{fast}, 2_{slow}, 3, and 4 provide a unique and probably complete "kinetic signature" (four rates and five amplitudes) of the dynamics of muscle fiber function. Each of these five phases arise either from a primary step in the cross-bridge cycle or from compliance-linked (spring-like) properties of cross-bridges (Davis, 2000). Of all the phases, only the fastest two are compliance related. Phase 1 provides a measure of cross-bridge elasticity (instantaneous stiffness), while the slower, kinetically controlled phase 2_{fast} is a measure of cross-bridge viscoelasticity (Davis, 1999; Davis and Harrington, 1993). The other H-S phases 2_{slow}, 3, and 4 are all cross-bridge cycle related. Each of these phases originates from one primary step in the cross-bridge cycle that is linked by different degrees (i.e., steady-state or kinetically coupled) to upstream and downstream steps in the cycle. In the simplified cross-bridge cycle shown in Scheme 1, M is myosin, A is actin, T is ATP, D is ADP, and P is P_i.

Indications are that phase 2_{slow} is linked to de novo tension generation and the creation of a primary force-generating state AMD* in step 7 (Davis and Harrington, 1993; Davis and Rodgers, 1995b); phase 3 to the actin-catalyzed release of phosphate from myosin and step 5 (Davis and Rodgers, 1995b); and phase 4 to the sequential functioning of the two heads of myosin where binding of the second head is prevented when the first head is strongly bound to actin, but has not yet passed through step 7 to generate force (Davis, 1998; Davis and Rodgers, 1995a).

In this paper we use both rabbit psoas type IIb and soleus type I fibers to study the consequences of RLC phosphorylation. In maximally Ca^{2+}-activated fibers, we find that phosphorylation partially reverses the inhibitory effect of 2,3-butanedione monoxime (BDM) on fiber tension by increasing phosphate release from actin-attached cross-bridges. This provides fresh insight into mechanism because the associated large increase in tension is observed in maximally Ca^{2+}-activated fibers, an activation state not normally associated with phosphorylation-induced increases in tension (Sweeney et al., 1993). Thus, increases in tension mediated by RLC phosphorylation appear to function independently of the state of the Ca^{2+} troponin/tropomyosin regulatory switch.

Small L-jump step-stretch experiments on single skinned fibers show for the first time that RLC phosphorylation causes a reduction in the normalized amplitudes of phase 3, and to a lesser extent phase 2_{slow}. No obvious changes in rates are observed. The overall consequence of these two changes is therefore to depress the amplitude of the trough-to-peak excursion producing the delayed rise in tension or stretch activation response. Taken together with the reversal of BDM inhibition by phosphorylation, changes in the L-jump kinetics and the increase in isometric tension at sub-maximal levels of activation, we propose that RLC phosphorylation up-regulates phosphate release from actin-attached myosin cross-bridges (step 5) to increase the flux of cross-bridges through phosphate release (phase 3) and on tension generation (phase 2_{slow}) (Davis, 1998; Davis and Harrington, 1993; Davis and Rodgers, 1995a; Davis and Rodgers, 1995b). Even though the site of phosphorylation is on the lever arm segment of the myosin head, there appears to be little change in normal (phase 1) and viscoelastic (phase 2_{fast}) stiffness of the cross-bridge.

$$\begin{array}{ccccccccc} & & & & 3 & & & & \\ & & & & \mathrm{MT} \leftrightarrows \mathrm{MDP} & & & & \\ & & & & & & & & \\ & & & & 2 \Downarrow \quad 4 \Downarrow & & & & \\ & & 1 & & & 5 & 6 & 7 & 8 \\ \mathrm{AM} + \mathrm{T} & \leftrightarrows & \mathrm{AMT} & & \mathrm{AMDP} & \leftrightarrows \mathrm{AMD} + \mathrm{P} & \leftrightarrows & \mathrm{AMD} & \leftrightarrows \mathrm{AMD}^* \leftrightarrows \mathrm{AM} + \mathrm{D} \end{array}$$

Scheme 1

MATERIALS AND METHODS

L-jump experiments

Rabbits were sacrificed under NHLBI Animal Care and Use Protocol 9CB-2. Fiber bundles of psoas muscle were prepared and chemically skinned (Davis and Harrington, 1993). Aluminum T-clips were used to attach the fiber to Invar mounting hooks in the tension transducer cell. Relaxing and preactivating and activating solutions of 0.2 M ionic strength are described elsewhere (Davis and Harrington, 1993). The activating solution (7.39 mM $MgCl_2$, 5.52 mM vanadium free ATP, 20 mM CaEGTA, 20 mM creatine phosphate, 15 mM disodium glycerol 2-phosphate and 1 mg ml^{-1} of creatine phosphokinase at pH 7.1 at 20°C) was modified to contain either 1or 5 mM added P_i. This was achieved by substituting equal concentrations of glycerol 2-phosphate buffer with NaH_2PO_4 (Davis and Rodgers, 1995b). Solutions with submaximal concentrations of Ca^{2+} were prepared by mixing phosphate containing activating and relaxing solutions in appropriate ratios. Resultant pCa values were calculated using the program MaxChelator (http://www.stanford.edu/~cpatton/maxc.html) (Bers et al., 1994).

The apparatus used to record the tension transients is described briefly, with details presented elsewhere (Davis and Harrington, 1993; Davis and Rodgers, 1995a). A model 407A (Cambridge Technology Inc., Cambridge, MA) fast capacitor-based force transducer with a resonant frequency of 12 kHz, 100 μs rise time and compliance of 0.1 μm g^{-1} was used for all tension measurements. An ergometer (model 300S, Cambridge Technology Inc.) was set to apply small L-jump stretches with a 100% rise time of 180 μs to the fiber. Voltage output from the force transducer amplifier and the detector measuring the position of the first order of the sarcomere diffraction pattern was recorded on a dual time base, four-channel digital oscilloscope (Integra 20, Nicolet Instrument Corporation, Madison, WI). Tension and sarcomere length changes were simultaneously recorded as 50,000 12-bit data points at fast rates of 20 μs per point, and slow rates of 200 μs for fast, and 400 μs per point for slow fibers. Methods of time base selection, data conditioning, and nonlinear least-squares analysis (Johnson and Frasier, 1985) used to determine the nine H-S kinetic constants are described in detail elsewhere (Davis, 2000).

RLC phosphorylation

A cloned human skeletal/cardiac MLCK (Davis et al., 2001) was used to phosphorylate single skinned rabbit psoas and soleus fibers. The enzyme was purified to homogeneity using FLAG-tag affinity chromatography (Sigma-Aldrich, St. Louis, MO), thus eliminating the possibility of contaminant kinase or phosphatase activities. The steady-state V_{max} value of 115 pmol min^{-1} ng^{-1} and K_m value of 17 μM are similar in value to that obtained for the enzyme purified to homogeneity from skeletal muscle tissue. The enzyme is specific for the RLC and unlike the smooth muscle isoforms, does not bind to the proteins of the fiber (Lin et al., 1997). Note that there is a recent report that MLCK binds weakly to actin filaments at low ionic strength and inhibits the movement of myosin in the in vitro motility assay (Fujita et al., 1999). We consider this observation irrelevant to our kinetic experiments because fiber V_{max} (the fiber equivalent of velocity in the in vitro motility assay) is unaffected either by RLC phosphorylation or by the addition of high concentrations of MLCK (0.12 μM) (Persechini et al., 1985).

Fibers prepared with our skinning and storage procedures show undetectable endogenous levels of RLC phosphorylation. To switch the RLC in these fibers to their phosphorylated state(s), we developed a method to fully activate the kinase with the fiber locked in a low-tension state. This was achieved using BDM to suppress tension while simultaneously phosphorylating the RLC with kinase. With fast fibers, 7.5 mM BDM was used to suppress tension, while 0.1 μM MLCK and 1.0 μM calmodulin were added to the standard activating solution to phosphorylate the RLC at 5°C. Fifteen minutes was sufficient to switch states. For slow fibers, BDM, kinase and calmodulin concentrations were doubled and the temperature increased to 20°C. Fifteen minutes was allowed to switch the non-phosphorylated pair of slow RLC to their fully phosphorylated states (non-phosphorylated forms P1 and P2 to phosphorylated forms P3 and P4 (Westwood et al., 1984)).

Single fibers were assayed to determine the level of RLC phosphorylation before, during, and after MLCK treatment. In each case, segments (≈3 mm) of fiber were assayed after the selective extraction of the light chains (Craig et al., 1987). The two fast and four slow RLC species were separated by glycerol-PAGE (Perrie and Perry, 1970). Gels were silver stained and scanned on a calibrated gel scanner. Scans were quantitated on a Macintosh computer using the public domain program NIH Image (available on the Internet at http://rsb.info.nih.gov/National Institutes of Health-image/).

Experimental procedures

Single skinned fibers ≈6 mm in length were used in the experiments. Aluminum T-clips were placed ≈3 mm apart leaving a free tail extending from one of the clips. This tail segment was cutoff and assayed for RLC phosphorylation level just before the fiber was loaded into the 40-μl trough of the L-jump apparatus containing relaxing solution. Solution changes in the trough were performed by applying a vacuum to one end of the trough while pipetting in the replacement solution at the other. Usually 1 ml of each solution was flowed slowly past the fiber. The fiber was first washed with relaxing solution, followed by the preactivating solution and then left for 5 min at 5°C to equilibrate. Submaximal activation solutions were prepared by mixing activating and relaxing solutions in a fixed ratio for all the experiments in a series. Before the experiments, the ratios necessary to achieve ≈50% activation for fast fibers at 5°C and 20% activation for slow fibers at 20°C were determined. Fiber activation was achieved by flowing the appropriate chilled solution past the fiber while simultaneously switching the cell's thermoelectric temperature regulator to the temperature of the experiment. Fiber tension was continuously monitored on a chart recorder. The Brenner protocol, in which sarcomere stability is preserved by releasing the fiber at low load and restretching it rapidly, was generally used (Brenner, 1983). Because a rotary rather than linear L-jump motor was used, the fiber swings through the solution with a stirring motion facilitating diffusion of proteins and metabolites in and out of the fiber. Great care was always taken to ensure that the fiber was in a steady-state at the point when the L-jump was applied (Davis, 2000). This required that the 10 20-s tension transients be collected over 4- and 10-min time periods for fast and slow fibers, respectively. The first and last tension transients were compared as a control for any untoward changes in fiber stability or state that might have occurred during the time course of the experiment from fiber damage, BDM and/or MLCK contamination, etc. RLC phosphorylation was initiated by washing in 200 μl of the appropriate BDM, MLCK and calmodulin containing activating solution. When the phosphorylation was complete, the fiber was washed slowly with 25 volumes the same cold, partial activation solution used to determine the pre-phosphorylation tension transients. Once fiber temperature and tension had stabilized, 10 tension transients were recorded. Beyond the wash, the ≈2500-fold difference between the fiber volume and that of the trough will ensure that any residual fiber contaminants would diffuse out and not return. Time dependent changes were checked for by comparing the first and last tension transients of the series of 10. The likelihood that BDM, MLCK, and calmodulin might remain in the fiber and alter the post-phosphorylation kinetics seems remote. Tensions at full activation were recorded after washing in an aliquot of standard activating solution before the experiment was terminated with relaxing solution. The fiber was then removed from the apparatus, placed in a refrigerated dissecting dish containing relaxing solution at 5°C and the segment cut free of the T-clips. The RLC phosphorylation state of the fiber was then checked as described above.

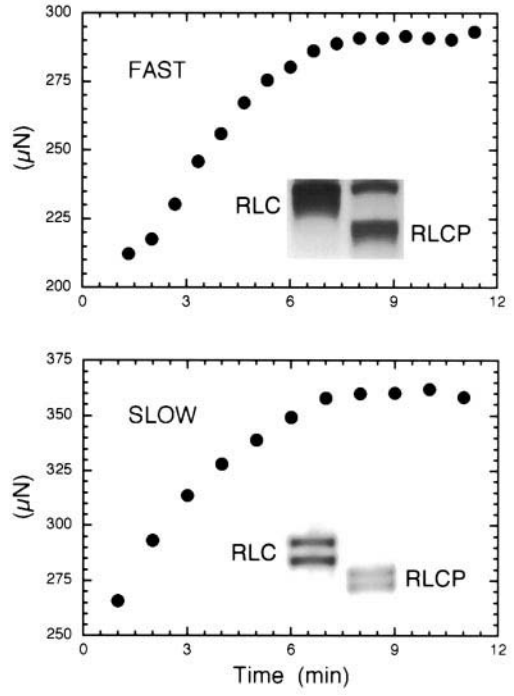

FIGURE 1 Tension increase during RLC phosphorylation of single, maximally Ca^{2+}-activated fast and slow fibers in the presence of BDM. RLC phosphorylation by Ca^{2+} calmodulin-activated MLCK was performed in the presence of BDM to depress fiber tension during the reaction. Isometric tension increases by a similar ≈40% in both fiber types. Gel analysis of single fibers segments taken at the start and end of treatment show a switch of the single RLC of type IIb fast fibers and the pair of RLC of type I slow fibers from the non-phosphorylated to phosphorylated states. Data from three separate experiments were averaged. See text for differences in the conditions used to phosphorylate fast and slow fibers.

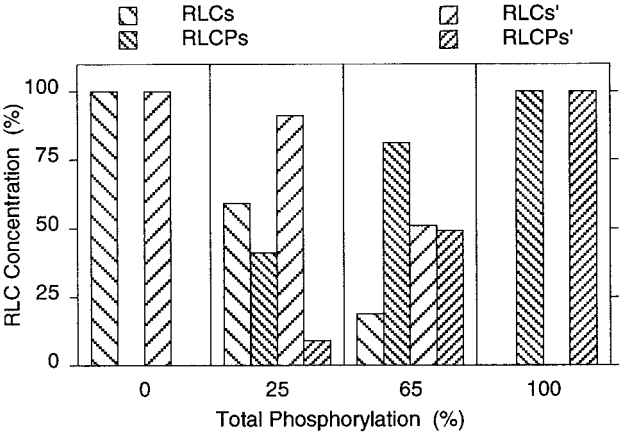

FIGURE 2 The two slow RLC isoforms of slow type1 fibers phosphorylate at different rates. Relative concentrations of the P1 (RLCs), P2 (RLCs′), P3 (RLCPs), and P4 (RLCPs′) in non-phosphorylated, part-phosphorylated, and fully phosphorylated fibers are shown. The slow migrating P1 RLC is phosphorylated ≈4-fold faster than the P2 RLC isoform. Both isoforms are generally present in similar amounts. These data were obtained from quantitative scans of silver-stained gels similar to and including those shown in the lower panel of Fig. 1.

RESULTS

RLC phosphorylation

Both fast and slow fibers prepared by our skinning procedure routinely show undetectable levels of endogenous RLC phosphorylation. To phosphorylate the RLC in these fibers, Ca^{2+} is required to activate the added calmodulin-MLCK complex. An unwanted consequence of the presence of the Ca^{2+} is that the fibers are fully activated with tension at a maximum. As detailed in Materials and Methods, we minimize tension-related fiber damage by a method that allows full activation of the added kinase by Ca^{2+} while maintaining the fiber in a low tension state with BDM. Gel insets to the panels of Fig. 1 show the complete switch between the non-phosphorylated and phosphorylated forms of the RLC for both fiber types. Fast, type IIb fibers from rabbit psoas muscle have a single RLC species. Slow, type I fibers from rabbit soleus muscle have two species of RLC. In this instance, the two non-phosphorylated forms (P1 and P2) are switched to their respective phosphorylated forms (P3 and P4) (Westwood et al., 1984).

Tension increases with RLC phosphorylation in BDM inhibited but fully Ca^{2+}-activated fibers

Tension records in the two panels of Fig. 1 show an ≈40% increase as RLC phosphorylation progresses with time, demonstrating that the tension of fully Ca^{2+}-activated, but BDM-inhibited, fibers can increase further on phosphorylation. Intermediate phosphorylation states of the RLC were determined during the rise in tension in parallel experiments under like conditions, but without monitoring tension. The results indicate roughly parallel increases in both fiber tension and RLCP content and also show that the two slow fiber RLC isoforms are phosphorylated at different rates (see below).

In fast fibers, the tension record shows a lag phase at the start as MLCK, calmodulin, and calcium penetrate the fiber. This phase is followed by a steady-state linear increase in tension (equivalent to the linear, zero-order initial rates measured to determine the classical Michaelis-Menten kinetic parameters) before tailing off to a plateau tension at full phosphorylation. The form of the tension rise is different in slow fibers. Here, the lag phase following the initiation of the phosphorylation reaction at time 0 is masked by the speed of the reaction. The rise in tension is curved from start until the plateau value is approached asymptotically at full phosphorylation. No single linear steady-state phase like that seen with fast fibers is observed. A likely explanation for the difference between the fast and slow fibers phosphorylation kinetics is that tension rise in slow fibers is the product of two different phosphorylation rates (one fast, the other slow) of the P1 and P2 light chain species. This observation is confirmed by the data of Fig. 2 that show that

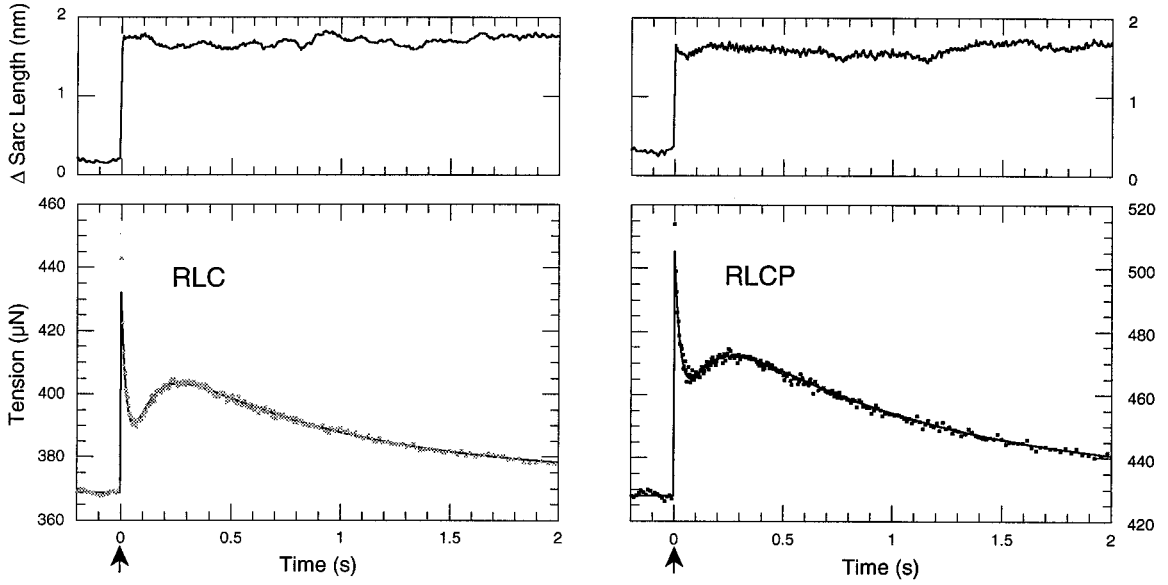

FIGURE 3 Effect of RLC phosphorylation on tension transients caused by a small step-stretch of a partially Ca^{2+}-activated fast, type IIb fiber. A step-stretch of 1.5 nm/half sarcomere was applied at time 0 (*arrow*). Ten consecutive tension and sarcomere length-change transients were averaged to improve the signal to noise ratio. On RLC phosphorylation, fiber tension rose by 14.8% from its initial 50% activation level of 369 μN to 428 μN causing an increase in the size of the tension transient. Contributions of the H-S phases 1, 2_{fast}, 2_{slow}, 3, and 4 to the tension transients were determined by nonlinear least-squares analysis. The resultant fit to these data is drawn as a solid line through each data set. Sarcomere length (nm/half sarcomere) was stable during the tension transients with a small 15% increase in end-compliance following RLC phosphorylation. Averaged kinetic constants from this and seven other similar experiments are listed in Table 1 and are used in Fig. 5 to simulate the tension transients and component phases.

the slow migrating P1 (RLCs) isoform is phosphorylated some 4-fold faster than the P2 (RLCs′) isoform during the early stages of the reaction.

This reversal of the inhibition of tension by BDM offers new insights into the consequences of RLC phosphorylation on the contractile cycle. This is particularly so, because the mechanism of BDM-mediated inhibition of fiber tension is well understood and is apparently caused by an increase in the rate of ATP hydrolysis (step 3) and the simultaneous inhibition of phosphate release (Herrmann et al., 1992) from an actin-bound cross-bridge state (step 5) (Zhao et al., 1995). It is striking that tension increases are a similar 40% for both fiber types. This is particularly significant since fiber type, BDM concentration, and temperature are quite different in the two experiments. This provides a number of constraints on mechanism and could be worthwhile investigating in greater detail.

Changes in the L-jump kinetics on RLC phosphorylation

Small L-jump stretches were used to elicit the classic H-S tension transients from rabbit psoas fast fibers (type IIb) and rabbit soleus slow fibers (type I) with their RLC in the non-phosphorylated and phosphorylated states. Changes caused by phosphorylation were assessed from both functional and mechanistic perspectives. The H-S phases determined from L-jump experiments make it possible to pinpoint which component processes of the contractile cycle (Scheme 1) are modified by RLC phosphorylation.

Experimentally, it is essential to select conditions so that all nine kinetic constants that govern the complete time course of the tension transient can be unambiguously determined for fast and slow fibers in both their RLC and RLCP states. To do this, we selected a particular temperature for the experiment such that the rates of the four phases are well separated from one another. The basis for this strategy is that each phase exhibits a different temperature sensitivity or Q_{10} value.

Fast fibers at submaximal activation

L-jump experiments on rabbit psoas fast type IIb fibers were performed at 5°C to optimize analysis. The activating solution contained 1 mM added phosphate and sufficient calcium to reach ≈50% of the maximal isometric tension in non-phosphorylated fibers. In each experiment fiber type and phosphorylation state were monitored by glycerol gel analysis as shown in the inset to Fig. 1. The added phosphate serves to buffer the phosphate concentration throughout the fiber and approximates the normal physiological concentration in muscle.

Switching the RLC state from zero to full phosphorylation in contracting single skinned fibers causes a modest but typical 14.9% increase in isometric tension (Persechini et al., 1985). Representative tension and sarcomere length

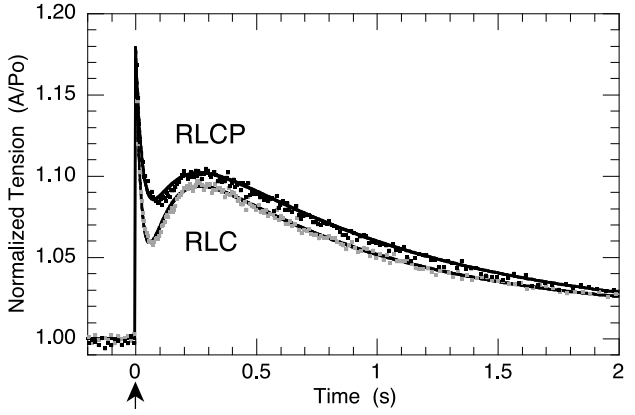

FIGURE 4 Effect of RLC phosphorylation on normalized tension transients caused by a small step-stretch of a partially Ca^{2+}-activated fast, type IIb fiber. These are the same data as in Fig. 3, but are normalized to isometric tension to highlight changes in the tension transient that are not proportional to isometric tension. A L-jump of1.5 nm/half sarcomere was applied at time 0 (*arrow*). Note the reduction in the size of the pulse-like delayed rise in tension on phosphorylation. The fit to the H-S phases 1, 2_{fast}, 2_{slow}, 3, and 4 was determined by nonlinear least-squares analysis and is drawn as a solid line through each data set.

transients are shown in Fig. 3. The observed 14% increase in end-compliance of the fiber is small and will have no effect on the rate constants and amplitudes determined by nonlinear least-squares analysis (Davis, 2000). The overall size of the tension transient increases in approximate ratio to the increase in isometric tension. As is evident in Fig. 3, sarcomere length is stable after the initial step increase synchronous with the 1.5 nm/half-sarcomere L-jump. Fig. 4 shows the same transients normalized to isometric tension. This serves to factor out increases in amplitude that are proportional to the increase in fiber tension caused by RLC phosphorylation. These normalized tension transients serve to highlight the phosphorylation-induced changes in the form (shape) of the tension transients. The rise in tension synchronous with stretch (phase 1) and the immediate fall in tension in the first few milliseconds following this (phase 2_{fast}) superimpose and indicate little change in either fiber elasticity or viscoelasticity, respectively. Divergence of the transients in the 50-ms time domain indicates a decrease in the amplitude of phase 2_{slow}, while the decrease in the magnitude of the delayed rise in tension peaking at 250 ms results primarily from a decrease in the amplitude of phase 3. The convergence and final superimposition of the two traces in the one second and longer time domains is due to little change in the kinetics of phase 4. The feature of note is that the trough-to-peak rise in tension leading up to the delayed rise in tension peak is sharper and larger in RLC-containing than in RLCP-containing fibers.

Quantitative analysis is achieved by subdividing the entire tension transient into the classical H-S phases by nonlinear least-squares analysis. The fit to phases 1, 2_{fast}, 2_{slow}, 3, and 4 are drawn as a solid lines though the data points of the tension transients of Figs. 3 and 4. Table 1 summarizes averaged kinetic constants (rates and amplitudes) from eight single fibers including the one depicted in Figs. 3 and 4. On phosphorylation, the absolute (actual) amplitudes are ≈15% larger than the normalized values in Table 1. Only two of the nine constants that govern the time-dependent changes in tension of a muscle fiber are significantly altered by RLC phosphorylation. Decreases in the amplitudes of phase 3, and to a lesser extent phase 2_{slow}, account for the change in the form (shape) of the delayed rise in tension on RLC phosphorylation. Fig. 5 illustrates just how large the changes in the amplitudes of phases 2_{slow} and 3 in fact are. In this figure, averaged kinetic constants from Table 1 are used to simulate the exponential time courses of phases 2_{fast}, 2_{slow}, 3, and 4. Substantial change is limited to the time courses of phase 3 and to a lesser extent phase 2_{slow}. Phases 1, 2_{fast}, and 4 match each other in the two plots. The superimposition of a series of exponential phases each with an origin at zero time is a signature characteristic of small-perturbation relaxation kinetic experiments in which the kinetics are either first or pseudo first-order (Davis, 2000).

TABLE 1 Effect of RLC phosphorylation on the nine Huxley-Simmons kinetic constants that govern the response of a 50% Ca^{2+}-activated fast (type IIb) muscle fiber to a small step-stretch

	Rate (s^{-1})		Normalized amplitude (A/Po)	
H-S phase	RLC	RLCP	RLC	RLCP
Phase 1			0.278 ± 0.008	0.267 ± 0.011
Phase 2_{fast}	1146 ± 242	1212 ± 183	−0.108 ± 0.004	−0.089 ± 0.005
Phase 2_{slow}	36.8 ± 3.8	43.0 ± 4.4	−0.229 ± 0.017	−0.157 ± 0.006
Phase 3	12.1 ± 0.8	9.0 ± 0.7	0.195 ± 0.021	0.117 ± 0.010
Phase 4	1.19 ± 0.13	1.09 ± 0.03	−0.124 ± 0.005	−0.127 ± 0.004

Data were obtained from L-jump experiments on eight individual fibers including that of Figs. 3 and 4. Decreases in the amplitudes of phase 3 (to 60%) and to a lesser extent phase 2_{slow} (to 69%) result from RLC phosphorylation, while fiber tension rose a modest 14.9%. Fig. 5 shows tension transients and component phases simulated from these averaged data. Error bounds are S.E.M. computed when the 8 data sets were averaged.

Slow fibers at submaximal activation

L-jump experiments on rabbit soleus type I slow fibers were performed at 20°C to optimize resolution of the H-S kinetic phases. Sufficient calcium was added to reach ≈20% of the maximal isometric tension in the initial non-phosphorylated state. A difficulty unique to the analysis of the L-jump kinetics in rabbit slow fibers is that they oscillate spontaneously when activated (Steiger, 1977). The phenomenon is particularly acute in tension and sarcomere length records from partially Ca^{2+}-activated fibers. Fig. 6 *C* shows that oscillations are present even after averaging tension transients from 11 fibers. As with fast fibers, an activating solution with 1 mM added phosphate was used in these initial experiments. Later, an activating solution with 5 mM

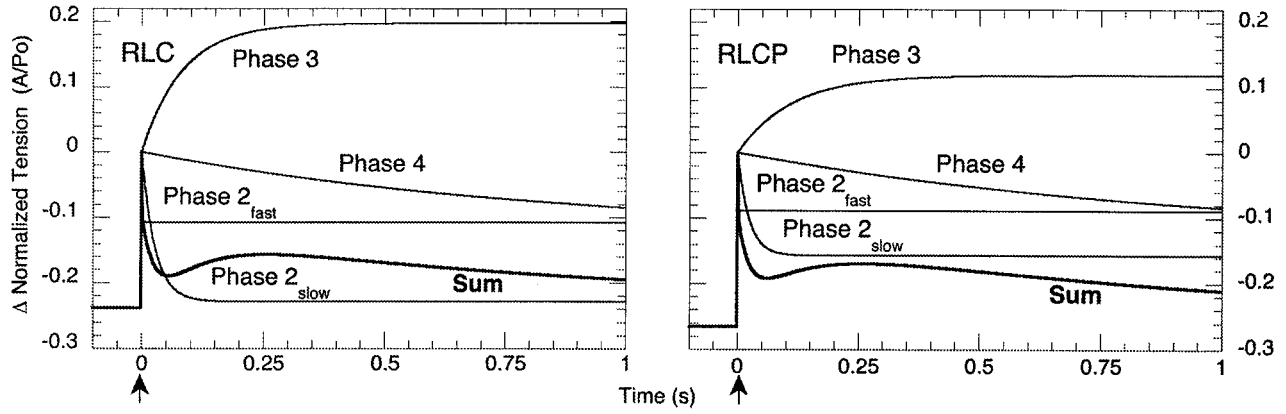

FIGURE 5 Simulated time courses of the L-jump tension transients and their component phases 1, 2_{fast}, 2_{slow}, 3, and 4 before and after RLC phosphorylation of fast, type IIb fibers. Changes in the kinetics on phosphorylation are limited to a 40% decrease in the amplitudes of phase 3 and 31% for phase 2_{slow}. Simulations were performed using the program Kaleidagraph (Synergy Software, Reading, PA) and the nine kinetic constants (from 8 fibers) listed in Table 1. An L-jump of 1.5 nm/half sarcomere was applied at time 0 (*arrow*).

added P_i was used to further reduce the oscillations. Even with 5 mM P_i, oscillations are still evident in the low tension RLC trace of Fig. 6 *B*. Increasing the phosphate concentration to 5 mM causes a small decrease in fiber tension and a slight increase of the rate of phase 3. From the perspective of our experiments, the overall cross-bridge cycle is little affected by changing the concentration of phosphate. The effect of increasing the phosphate concentration is to slow the release of phosphate (by mass action) from the cross-bridge at step 5, thereby reducing the overall number of cycling cross-bridges and thus tension. Note that rate of phase 3 is an apparent rate constant or relaxation time and, as such, is not a measure of the rate of phosphate release (Davis, 2000). Thus the cross-bridge cycle and RLC phosphorylation regulation mechanisms are minimally affected by changing the concentration of P_i.

Fig. 6 *A* shows that tension increases a dramatic 2.5-fold, from 22% to 56% of the maximal value, upon phosphorylation. This is due in part to the 20°C temperature (compared to 5°C used in our fast fiber experiments), but also appears to be an intrinsic property of type I slow fibers. Fig. 6 shows that switching the RLC state from zero to full phosphorylation alters the dynamics of contraction. As with fast fibers (Fig. 4), the trough-to-peak excursion leading up to the delayed rise in tension/stretch activation response is more pronounced in non-phosphorylated fibers. One difference, however, is that the delay peaks at a higher normalized tension in RLC-containing fibers, which is the inverse of the fast fiber case. Examination of Fig. 6 B shows that the two normalized tension transients appear to superimpose during phases 1, 2_{fast}, and 2_{slow}, indicating little change in these kinetic parameters. Data in Table 2 show, however, that there are changes in the normalized amplitudes phases 1, 2_{fast}, and 2_{slow} on RLC phosphorylation. Nevertheless, these differences are eliminated if the positive and negative amplitudes of phases 1, 2_{fast}, and 2_{slow} are added together. The net result is that the endpoint of phase 2 (the classical H-S T_2 (Huxley and Simmons, 1971)) is unchanged at 96.5% and 96.3% of isometric tension in both RLC- and RLCP-containing fibers, respectively. Divergence of two transients from this point at 500 ms on, is primarily due to the decrease in the amplitude of phase 3 associated with RLC phosphorylation. The form of the two traces from 3 s out is due to a decrease in the amplitude and rate of phase 4 upon phosphorylation. Quantitative analysis of these data, summarized in Table 2, matches these observations. Note that the absolute (actual) amplitudes in the table are some 2.5-fold greater than the normalized amplitudes after RLC phosphorylation. The primary effect of phosphorylation on the delayed rise in tension is a 26% decrease in the normalized amplitude of phase 3 and possibly a small drop in the rate of phase 2_{slow}. Larger 0.8% stretches result in tension transients closer in form to the fast fiber tension transients of Fig. 4 (Davis et al., 2001).

Tension transients caused by stretch of a fast fiber (Fig. 4) seldom if ever fall below the steady-state isometric tension level. That is, the H-S T_2 curve (the drop in tension due to phase 2) remains above P_0. However, as we confirm, the type I fiber response is not only slower in rate, but as can be seen in Fig. 5, tension frequently drops to T_2 values below the steady-state isometric tension (Steiger, 1977). This peculiarity of slow fibers could have important functional consequences for muscles subjected to stretch under load. An example would be opposing muscle groups that alternately stretch and contract against each other.

DISCUSSION

Nearly all kinetic experiments on the consequences of RLC phosphorylation have been pre-steady-state experiments

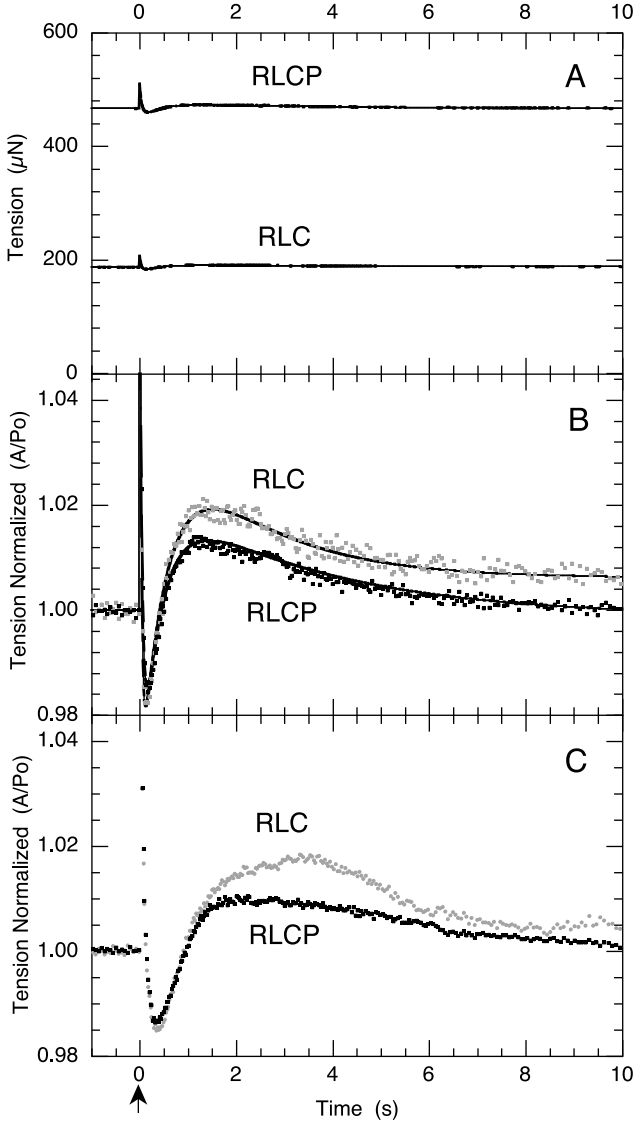

FIGURE 6 Effect of RLC phosphorylation on tension transients caused by a small step-stretch of a partially Ca^{2+}-activated slow, type I muscle fiber. An L-jump of 1.5 nm/half sarcomere was applied at zero time (*arrow*). (*A*) The pre-jump isometric tension increased dramatically from 207 μN to 517 μN (22% to 56% of maximal tension) on phosphorylation. The concentration of added phosphate was 5 mM and tension transients from eight fibers were averaged. (*B*) Same data as in *A*, but normalized to isometric tension. Note the reduction in the size of the pulse-like delayed rise in tension on phosphorylation. Solid lines drawn through these averaged data from 8 fibers are the nonlinear least-squares fits to the H-S L-jump phases 1, 2_{fast}, 2_{slow}, 3, and 4. The amplitude of phase 3 alone declines significantly. Kinetic constants obtained from the analysis are listed in Table 2. (*C*) Normalized tension transients before and after phosphorylation recorded with a more physiological 1 mM added phosphate. Oscillations in tension, particularly evident in the low tension RLC trace, preclude analysis. Otherwise changes in the kinetics are similar in form to *B*. Data from 11 fibers were averaged.

that induce tension transients either by initiating or terminating contraction. The time course of the tension change is then analyzed. Under ideal circumstances pre-steady-state kinetic experiments can provide information about the rise and fall in the concentrations of intermediates of the contractile cycle up to, but not beyond the rate-limiting step (Gutfreund, 1995). This is because faster steps beyond the rate-limiting step occur at rates governed by the upstream slow step and not by their own rate constants. Included in this class of experiment are the activation of contraction by the release of caged ATP, the related recovery of tension (k_{TR}) after a fast restretch of a transiently shortened fiber and the sequestration or release of Ca^{2+} by photolysis of a caged chelator (Metzger et al., 1989; Patel et al., 1998; Sweeney and Stull, 1990). The L-jump step-stretch experiments we perform belong to a different category. The power of these small perturbation relaxation experiments is that they probe steps both before and after the rate-limiting step (Davis, 2000). The requirement is that, unlike pre-steady-state experiments, the concentrations of intermediates of the steady-state cross-bridge cycle are little changed. As detailed in the Introduction, changes in the various L-jump H-S phases correlate with and measure the interconversions of individual ATPase and mechanical intermediates of the isometric contractile cycle. Our experiments show that L-jump tension transients are altered in a particular way by phosphorylation.

Functional consequences of RLC phosphorylation on the L-jump kinetics

Greatest emphasis will be placed on the fast fiber data for the following reasons: First, most of the background research on the biochemistry and mechanics of muscle contraction have been performed on fast fibers. Second, the quality of our fast fiber data is higher than the slow fiber data where experiments were plagued by spontaneous oscillations in tension and sarcomere length.

The dominant change in the form of the tension transients common to both fiber types, occurs in the delayed rise in tension. Non-phosphorylated fibers typically show a marked rebound of tension following a step-stretch. In phosphorylated fibers isometric tension is higher, but the size of the rebound peak is reduced. This change in the form of the transient is common to both fast and slow fibers. The primary cause is the phosphorylation-induced decrease in the normalized amplitude of phase 3. In fast, and possibly in slow fibers, there is also a lesser decrease in the normalized amplitude of phase 2_{slow}. Rates change little, except possibly in slow fibers where the rate of phase 2_{slow} appears to increase, but this could be a secondary effect caused by the strain sensitivity of phase 2_{slow} responding to the large increase in fiber tension (Davis, 1998; Huxley and Simmons, 1971). With regard to peak height of the delayed rise in tension, the larger the amplitude of phase 2_{slow}, the deeper the trough before the peak; the larger the amplitude of phase 3, the greater the height of the peak itself. The phenomenon described is best seen in Fig. 5, where RLC-

TABLE 2 Effect of RLC phosphorylation on the nine Huxley-Simmons kinetic constants that govern the response of a 20% Ca^{2+}-activated slow (type I) muscle fiber to a small step-stretch

	Rate (s^{-1})		Normalized amplitude (A/Po)	
H-S phase	RLC	RLCP	RLC	RLCP
Phase 1			0.120 ± 0.001	0.100 ± 0.001
Phase 2_{fast}	331 ± 26	192 ± 18	−0.034 ± 0.001	−0.023 ± 0.001
Phase 2_{slow}	29.2 ± 0.49	20.6 ± 0.26	−0.121 ± 0.002	−0.114 ± 0.001
Phase 3	1.80 ± 0.11	2.33 ± 0.15	0.081 ± 0.002	0.060 ± 0.002
Phase 4	0.516 ± 0.021	0.293 ± 0.012	−0.040 ± 0.001	−0.025 ± 0.001

Data are from the analysis of the two tension transients (average of 8 fibers) of Fig. 6, *A* and *B*. RLC phosphorylation causes a 2.5-fold increase in fiber tension from 22% to 56% (207 μN to 517 μN) of the maximal value. Changes in the kinetics are limited to a 26% decrease in the amplitude of phase 3 and a 29% decrease in the rate of phase 2_{slow}. See text for other changes. Error bounds are 67% confidence limits returned on the nonlinear least-squares fit to the averaged data (Johnson and Frasier, 1985).

containing fibers generate a prominent stretch activation/delayed rise in tension peak. Thus, stretch activation, or the delayed rise in tension, is effectively damped by phosphorylation of the RLC in both fast type IIb and slow type I fibers.

A lack of significant change in phases 1 and 2_{fast}, and thus the instantaneous and damped stiffness of our benchmark fast fibers, indicates little change in the mechanical properties of the cross-bridge. Thus phosphorylation of the RLC on the neck of the myosin molecule leaves the mechanical properties of the lever arm unchanged.

The site of regulation of the contractile cycle by RLC phosphorylation

There is established experimental evidence to show that RLC phosphorylation functions by enhancing the rate of formation of force generating state(s) (Metzger et al., 1989; Sweeney and Stull, 1990). The partial reversal of the BDM inhibition of fiber tension by RLC phosphorylation that we observe places some interesting constraints on this mechanism. Interpretation is simplified because tension inhibition by BDM causes cross-bridges to accumulate in a specific weakly bound A–M·ADP·P_i state. RLC phosphorylation causes a 40% reversal of this step-specific inhibition. BDM serves as an uncompetitive inhibitor causing a large increase in the equilibrium constant for ATP hydrolysis (step 3) while at the same time strongly inhibiting the actin-catalyzed release of phosphate (step 5) and subsequent tension generation (Herrmann et al., 1992). In Scheme 1, this results in a buildup in the concentration of the intermediates wedged between ATP hydrolysis (step 3) and phosphate release (step 5). EPR probe studies have shown that BDM inhibition leads to a buildup of actin attached cross-bridges that generate little or no tension with the catalytic domains of the myosin in a disordered state (Zhao et al., 1995). Thus, step 4 is strongly biased in the forward direction toward actin-attachment. Our proposal is that RLC phosphorylation functions to accelerate P_i release from this actomyosin products complex by relieving inhibition of step 5, thereby pinpointing the site of regulation.

Calcium regulation and RLC phosphorylation

One of the classic observations is that RLC phosphorylation causes a shift in the pCa vs. tension curve to the left and higher sensitivities (Persechini et al., 1985). In the experiments we have described, this phenomenon manifests itself as an increase in fiber tension in partially activated fast and slow fibers. The weakly bound state formed by BDM inhibition and thus the site of control by RLC phosphorylation, does not appear to be Ca^{2+} regulated. The first hint of this came from our experimental observations that RLC phosphorylation causes isometric tension to rise ≈40% in both fast and slow fibers inhibited by BDM, but with a high concentration of Ca^{2+} present. This contrasts markedly with normal fibers where RLC phosphorylation has no detectable effect on tension when the troponin/tropomyosin system is similarly saturated with Ca^{2+} (Persechini and Stull, 1984). There are other lines of evidence to suggest that the intermediate state associated with BDM inhibition is not Ca^{2+} regulated. For instance, pCa vs. tension curves differ little in form between BDM inhibited and control fibers (Brotto et al., 1995; Martyn et al., 1999). This lack of an effect on calcium sensitivity is in marked contrast to the phosphate mediated inhibition of the same step 5. Competitive inhibition by phosphate differs from the uncompetitive inhibition by BDM in that addition of the former causes a general reversal of the cross-bridge cycle rather than the forced accumulation of a particular intermediate. Increasing concentrations of P_i cause a marked shift of the pCa curve to the right, indicating a decreased sensitivity of fiber tension to Ca^{2+} regulation. The mechanism in this case likely functions via a P_i-mediated mass action reversal of earlier steps in the cycle including cross-bridge dissociation from actin (Millar and Homsher, 1990). Similarly, in uninhibited fibers, RLC phosphorylation would also appear to be linked to Ca^{2+} regulation. We can therefore subdivide the pathway

to tension generation associated with f_{app} (k_{TR}) of the models of Metzger et al. (1989) and Sweeney and Stull (1990) into two subcomponents: 1) an earlier group of Ca^{2+} regulated steps; 2) the later actin-catalyzed release of phosphate from the A–M·ADP·P_i state (the weakly bound or attached "A" state reviewed in Geeves (1991) regulated directly by RLC phosphorylation, but apparently unaffected by Ca^{2+}.

Differences between the mechanisms for the Ca^{2+}-mediated regulation of fiber tension and the phosphorylation-mediated regulation of fiber tension are supported by some other observations. The pattern of rate constant changes associated with the increase in tension on RLC phosphorylation and the increase in tension associated with increased Ca^{2+} activation appear different. Ca^{2+} activation causes the rate of phase 3 to increase with the extent of fiber activation (Steiger, 1977). RLC phosphorylation and the concomitant increase in tension, on the other hand, has little effect on the rate of phase 3. A slight decrease in rate from 12 to 9 s^{-1} is seen in fast fibers, while there is a slight increase of 1.83 to 2.4 s^{-1} in slow fibers.

The response we see in mammalian muscle fibers also differs from that observed in *Drosophila* indirect flight muscle, where mutating either or both the two RLC phosphorylatable serines to alanine inhibits the stretch activation response, presumably by locking the RLC in its non-phosphorylated state (Tohtong et al., 1995).

Possible mechanism to explain why RLC phosphorylation has no effect on tension and a large effect on k_{TR} at maximal activation

In an earlier paper, we proposed on the basis of laser temperature-jump experiments that the two heads of myosin function in a sequential and coordinated manner in maximally Ca^{2+}-activated fibers (Davis, 1998). Here we consider the possibility that this mechanism might offer an explanation as to why RLC phosphorylation has its greatest effect on pCa tension curves at low levels of activation and its greatest effect on pCa force-redevelopment (k_{TR}) curves at high levels of activation.

A characteristic of the second head mechanism is that it dominates function at full activation when the muscle is in an isometric steady state. Under these conditions the maximum number of cross-bridges are attached to actin and are generating force. The overall rate of the cross-bridge cycle is limited because the second head is blocked from interacting productively with actin while the first head is in a strongly actin-attached state. The consequence in Scheme 1 is that step 4 is slowed. Any increase in the rate of step 5 resulting from RLC phosphorylation would leave the overall flux through cycle and the P_i release step largely unaffected because the upstream steps would be inhibited and thus rate-limiting. On the other hand, the rate of tension redevelopment (k_{TR}) would occur at the maximum rate because high Ca^{2+} would maximize flux through the transitions it regulates (not shown in Scheme 1) by switching the regulatory proteins fully on. More importantly, myosin heads would be interacting for the first time with thin filaments sparsely populated with myosin heads and would not be down-regulated by the second head mechanism. The net result is that step 5 is once again rate-limiting, reestablishing control by RLC phosphorylation. At low levels of activation the converse applies. Tension is sensitive to RLC phosphorylation because the thin filaments are sparsely populated with myosin heads, increasing the probability of fast, first head attachment and thereby reestablishing step 5 as rate-limiting. Tension redevelopment (k_{TR}), on the other hand, is slow and insensitive to control by RLC phosphorylation because the calcium regulated steps are slow (low [Ca^{2+}]) and rate-limiting.

The mechanism we propose gives detail to the general "black box" mechanism put forward by Sweeney and Stull in which RLC phosphorylation progressively increases the rate of f_{app}. In their scheme, k_{TR} would increase in rate in proportion to f_{app} according to the relation $k_{TR} = f_{app} + g_{app}$ (Sweeney and Stull, 1990). Our mechanism provides a means to increase the rate of formation of the force generating state(s) (f_{app}) when the thin filament has a low density of newly attached myosin heads and is largely functioning under single or first turnover conditions.

Regulation of the contraction kinetics of oscillating muscles by RLC phosphorylation

Compared to the obvious functional consequences of increased tension accompanying RLC phosphorylation, the associated changes in the kinetics we described have the potential to influence the dynamic aspects of muscle function. The falloff in tension directly after fiber stretch followed by the transient reversal of this decline synchronous with the delayed rise in tension is a feature exploited in muscle groups that alternately stretch and contract against each other. Included are muscles responsible for locomotion, cardiac muscle and the indirect flight muscle of insects. In mammals, cardiac muscle is probably the most dependent on this property to increase oscillatory power (Davis et al., 2001; Poetter et al., 1996; Vemuri et al., 1999).

The effect of phosphorylation on the delayed rise in tension/stretch activation response of rabbit slow muscle is directly relevant to rabbit and human cardiac muscle because (within species) the β-myosins are identical in both tissues (Cuda et al., 1993). Recently we have addressed the role of RLC phosphorylation in the heart using larger, physiologically relevant L-jump stretches to highlight the qualitative relevance to cardiac function. (Davis et al., 2001). A compelling observation is that the kinetics of stretch activation (phase 3) in cardiac muscle correlates with heart rate of various animals (Steiger, 1977). This relationship holds in our experiments for the stretch activation

response in rabbit slow type I fibers where the H-S phase 3 has a rate of 1.5 s^{-1} at 20°C (adjusted to 1mM P_i). This rate is comparable to other apparent rate constants (3 s^{-1} process B [Wang and Kawai, 1997] and 3.85 s^{-1} k_{Pi} [Millar and Homsher, 1992]) describing the same process (Davis, 1998) under similar conditions. Assuming a range of 1–4 s^{-1}, conversion to frequency at 40°C (using a Q_{10} of 3 [Zhao and Kawai, 1994]) yields 86–344 beats/min. This is a reasonable match to the physiological heart rate of 130–325 beats/minute in the rabbit. Because the rate constant of stretch activation in rabbit slow fibers is commensurate with rabbit heart rate, the delayed tension that follows each stretch is available for work production at the end of each contraction cycle. Thus, an increase in oscillatory power is accomplished by reciprocally controlling tension and the stretch activation response through light chain phosphorylation (Davis et al., 2001).

RLC phosphorylation of insect flight muscle is likewise critical to the oscillatory power required for flight (Tohtong et al., 1995). However, whereas the amplitude of the stretch activation response is increased by phosphorylation in insect flight muscle, the reverse is true in mammalian slow fibers. Thus, in adapting the mechanics of wing beating to the vertebrate heart, evolution retained the "switch" but reversed the polarity.

Tension regulation in slow skeletal and cardiac muscle

We have shown that RLC phosphorylation results in a remarkably large 2.5-fold increase in fiber tension from 22% to 56% of the maximal Ca^{2+}-activated value in type I slow fibers. Corrected for temperature this is significantly larger than the 1.6-fold (20–33%) change recorded in recent experiments on fast, type IIb rabbit psoas fibers under matching conditions (Levine et al., 1998). While clearly having a role in slow muscle physiology, the effect is dramatic in the heart which normally functions at half-maximum activation. Thus RLC phosphorylation can modulate tension from close to zero to full power at a fixed level of Ca^{2+} activation. Our recent discovery of the gradient of RLC phosphorylation (high at the epicardial surface, low at the endocardial surface) and the consequences of RLC phosphorylation for cardiac mechanics are discussed in more detail elsewhere (Davis et al., 2001).

Different rates of phosphorylation for the two slow/cardiac RLC isoforms adds an extra level of complexity and control to the mechanism since the P1 (RLCs) isoform phosphorylates at least 4-fold faster than the P2 (RLCs′) isoform. In our experiments with slow skeletal muscle fibers, both these isoforms are present in roughly equal amounts. It is not known whether this is true for all species or even if the isoform distribution is graded in the heart. Physiological function might be fully served by having a fraction of the RLC population in a fiber phosphorylate rapidly relative to the rest. RLC phosphorylation does not change the H-S rate constants, only amplitudes. This limitation could present a synchronization problem for muscles which function over a wide range of oscillatory frequencies. There are, however, other available mechanisms to adapt rates to the speed of function. For example, the concentration of P_i in the fiber and the Ca^{2+} activation mechanism both alter the rate of phase 3 kinetics and thus the timing of the delayed rise in tension and could also serve to synchronize the kinetics to the rate of contraction.

CONCLUSION

We have presented evidence to show that RLC phosphorylation increases the number of cross-bridges entering the contractile cycle by up-regulation of actin-induced phosphate release from the weakly bound A–M·ADP·P_i state. On the basis of BDM inhibition data, we propose that this step is not regulated by Ca^{2+}. Equilibrium coupling between these two different regulation mechanisms appears to mediate the experimentally observed linkage between Ca^{2+} sensitivity and RLC phosphorylation. In accord with these observations there are no significant phosphorylation-induced changes in rates of the kinetic phases that comprise the H-S L-jump tension transients. The independent scaling of the amplitude of phase 3 (and to a degree phase 2_{slow}) relative to tension, elasticity, viscoelasticity and the amplitude of phase 4 does not seem to have a simple mechanism. One factor that links phases 2_{slow} and 3 is that both are on the direct pathway to tension generation. The reduction of the amplitude of phase 3 in both fiber types and of phase 2_{slow} in fast fibers underlies the phosphorylation-mediated depression of the delayed rise in tension, a property that has been shown to be important in the production of oscillatory power in the heart.

We thank Dr. James Sellers, who kindly supplied the calmodulin, and Dr. Steve O. Winitsky for comments on the manuscript.

REFERENCES

Adhikari, B. B., J. Somerset, J. T. Stull, and P. G. Fajer. 1999. Dynamic modulation of the regulatory domain of myosin heads by pH, ionic strength, and RLC phosphorylation in synthetic myosin filaments. *Biochemistry.* 38:3127–3132.

Bers, D. M., C. W. Patton, and R. Nuccitelli. 1994. A practical guide to the preparation of Ca^{2+} buffers. *Methods Cell Biol.* 40:3–29.

Brenner, B. 1983. Technique for stabilizing the striation pattern in maximally calcium-activated skinned rabbit psoas fibers. *Biophys. J.* 41: 99–102.

Brotto, M. A., R. T. Fogaca, T. L. Creazzo, R. E. Godt, and T. M. Nosek. 1995. The effect of 2,3-butanedione 2-monoxime (BDM) on ventricular trabeculae from the avian heart. *J. Muscle Res. Cell Motil.* 16:1–10.

Craig, R., R. Padron, and J. J. Kendrick. 1987. Structural changes accompanying phosphorylation of tarantula muscle myosin filaments. *J. Cell Biol.* 105:1319–1327.

Cuda, G., L. Fananapazir, W. S. Zhu, J. R. Sellers, and N. D. Epstein. 1993. Skeletal muscle expression and abnormal function of beta-myosin in hypertrophic cardiomyopathy. *J. Clin. Invest.* 91:2861–2865.

Davis, J. S. 1998. Force generation simplified: insights from laser temperature-jump experiments on contracting muscle fibers. *Adv. Exp. Med. Biol.* 453:343–351; discussion 351–352.

Davis, J. S. 1999. The Huxley-Simmons phase 2 and force generation: a comparative study. *Biophys. J.* 76:A269.

Davis, J. S. 2000. Kinetic analysis of dynamics of muscle function. *Methods Enzymol.* 321:23–37.

Davis, J. S., and W. F. Harrington. 1993. A single order-disorder transition generates tension during the Huxley-Simmons phase 2 in muscle. *Biophys. J.* 65:1886–1898.

Davis, J. S., S. Hassanzadeh, S. O. Winitsky, C. L. Satorius, H. Lin, R. Vemuri, H. Wen, and N. D. Epstein. 2001. The overall pattern of cardiac contraction depends on a spatial gradient of myosin regulatory light chain phosphorylation. *Cell.* 107:631–641.

Davis, J. S., and M. E. Rodgers. 1995a. Force generation and temperature-jump and length-jump tension transients in muscle fibers. *Biophys. J.* 68:2032–2040.

Davis, J. S., and M. E. Rodgers. 1995b. Indirect coupling of phosphate release and de novo tension generation during muscle contraction. *Proc. Natl. Acad. Sci. U.S.A.* 92:10482–10486.

Fujita, K., L. H. Ye, M. Sato, T. Okagaki, Y. Nagamachi, and K. Kohama. 1999. Myosin light chain kinase from skeletal muscle regulates an ATP-dependent interaction between actin and myosin by binding to actin. *Mol. Cell Biochem.* 190:85–90.

Geeves, M. A. 1991. The dynamics of actin and myosin association and the cross-bridge model of muscle contraction. *Biochem. J.* 274:1–14.

Grange, R. W., R. Vandenboom, and M. E. Houston. 1993. Physiological significance of myosin phosphorylation in skeletal muscle. *Can. J. Appl. Physiol.* 18:229–242.

Gutfreund, H. 1995. Kinetics for the Life Sciences: Receptors, Transmitters, and Catalysts. Cambridge University Press, Cambridge.

Herrmann, C., J. Wray, F. Travers, and T. Barman. 1992. Effect of 2,3-butanedione monoxime on myosin and myofibrillar ATPases: an example of an uncompetitive inhibitor. *Biochemistry.* 31:12227–12232.

Huxley, A. F. 1957. Muscle structure and theories of contraction. *Prog. Biophys.* 7:255–318.

Huxley, A. F., and R. M. Simmons. 1971. Proposed mechanism of force generation in striated muscle. *Nature.* 233:533–538.

Johnson, M. L., and S. G. Frasier. 1985. Nonlinear least-squares analysis. *Methods Enzymol.* 117:301–342.

Levine, R. J., R. W. Kensler, Z. Yang, J. T. Stull, and H. L. Sweeney. 1996. Myosin light chain phosphorylation affects the structure of rabbit skeletal muscle thick filaments. *Biophys. J.* 71:898–907.

Levine, R. J., Z. Yang, N. D. Epstein, L. Fananapazir, J. T. Stull, and H. L. Sweeney. 1998. Structural and functional responses of mammalian thick filaments to alterations in myosin regulatory light chains. *J. Struct. Biol.* 122:149–161.

Lin, P-J., K. Luby-Phelps, and J. T. Stull. 1997. Binding of myosin light chain kinase to cellular actin-myosin filaments. *J. Biol. Chem.* 272: 7412–7420.

Manning, D. R., and J. T. Stull. 1982. Myosin light chain phosphorylation-dephosphorylation in mammalian skeletal muscle. *Am. J. Physiol.* 242: C234–C241.

Martyn, D. A., C. J. Freitag, P. B. Chase, and A. M. Gordon. 1999. Ca^{2+} and cross-bridge-induced changes in troponin C in skinned skeletal muscle fibers: effects of force inhibition. *Biophys. J.* 76:1480–1493.

Metzger, J. M., M. L. Greaser, and R. L. Moss. 1989. Variations in cross-bridge attachment rate and tension with phosphorylation of myosin in mammalian skinned skeletal muscle fibers: implications for twitch potentiation in intact muscle. *J. Gen. Physiol.* 93:855–883.

Millar, N. C., and E. Homsher. 1990. The effect of phosphate and calcium on force generation in glycerinated rabbit skeletal muscle fibers: a steady-state and transient kinetic study. *J. Biol. Chem.* 265: 20234–20240.

Millar, N. C., and E. Homsher. 1992. Kinetics of force generation and phosphate release in skinned rabbit soleus muscle fibers. *Am. J. Physiol.* 262:C1239–C1245.

Moore, R. L., M. E. Houston, G. A. Iwamoto, and J. T. Stull. 1985. Phosphorylation of rabbit skeletal muscle myosin in situ. *J. Cell Physiol.* 125:301–305.

Patel, J. R., G. M. Diffee, X. P. Huang, and R. L. Moss. 1998. Phosphorylation of myosin regulatory light chain eliminates force-dependent changes in relaxation rates in skeletal muscle. *Biophys. J.* 74:360–368.

Perrie, W. T., and S. V. Perry. 1970. An electrophoretic study of the low-molecular-weight components of myosin. *Biochem. J.* 119:31–38.

Persechini, A., and J. T. Stull. 1984. Phosphorylation kinetics of skeletal muscle myosin and the effect of phosphorylation on actomyosin adenosinetriphosphatase activity. *Biochemistry.* 23:4144–4150.

Persechini, A., J. T. Stull, and R. Cooke. 1985. The effect of myosin phosphorylation on the contractile properties of skinned rabbit skeletal muscle fibers. *J. Biol. Chem.* 260:7951–7954.

Poetter, K., H. Jiang, S. Hassanzadeh, S. R. Master, A. Chang, M. C. Dalakas, I, Rayment, J. R. Sellers, L. Fananapazir, N. D. Epstein. 1996. Mutations in either the essential or regulatory light chains of myosin are associated with a rare myopathy in human heart and skeletal muscle. *Nat. Genet.* 13:63–69.

Rayment, I., W. R. Rypniewski, K. Schmidt-Base, R. Smith, D. R. Tomchick, M. M. Benning, D. A. Winkelmann, G. Wesenberg, and H. M. Holden. 1993. Three-dimensional structure of myosin subfragment-1: a molecular motor. *Science.* 261:50–58.

Steiger, G. 1977. Stretch activation and tension transients in cardiac, skeletal, and insect flight muscle. *In* Insect Flight Muscle. R. T. Tregear, editor. North Holland, Amsterdam. 221–268.

Sweeney, H. L., B. F. Bowman, and J. T. Stull. 1993. Myosin light chain phosphorylation in vertebrate striated muscle: regulation and function. *Am. J. Physiol.* 264:C1085–C1095.

Sweeney, H. L., and J. T. Stull. 1990. Alteration of cross-bridge kinetics by myosin light chain phosphorylation in rabbit skeletal muscle: implications for regulation of actin-myosin interaction. *Proc. Natl. Acad. Sci. U.S.A.* 87:414–418.

Tohtong, R., H. Yamashita, M. Graham, J. Haeberle, A. Simcox, and D. Maughan. 1995. Impairment of muscle function caused by mutations of phosphorylation sites in myosin regulatory light chain. *Nature.* 374: 650–653.

Trybus, K. M. 1994. Role of myosin light chains. *J. Muscle Res. Cell Motil.* 15:587–594.

Vemuri, R., E. B. Lankford, K. Poetter, S. Hassanzadeh, K. Takeda, Z. X. Yu, V. J. Ferrans, and N. D. Epstein. 1999. The stretch-activation response may be critical to the proper functioning of the mammalian heart. *Proc. Natl. Acad. Sci. U.S.A.* 96:1048–1053.

Wang, G., and M. Kawai. 1997. Force generation and phosphate release steps in skinned rabbit soleus slow-twitch muscle fibers. *Biophys. J.* 73:878–894.

Westwood, S. A., O. Hudlicka, and S. V. Perry. 1984. Phosphorylation in vivo of the P light chain of myosin in rabbit fast and slow skeletal muscles. *Biochem. J.* 218:841–847.

Xie, X., D. H. Harrison, I. Schlichting, R. M. Sweet, V. N. Kalabokis, A. G. Szent-Gyorgyi, and C. Cohen. 1994. Structure of the regulatory domain of scallop myosin at 2.8 Å resolution. *Nature.* 368:306–312.

Zhao, L., N. Naber, and R. Cooke. 1995. Muscle cross-bridges bound to actin are disordered in the presence of 2,3-butanedione monoxime. *Biophys. J.* 68:1980–1990.

Zhao, Y., and M. Kawai. 1994. Kinetic and thermodynamic studies of the cross-bridge cycle in rabbit psoas muscle fibers. *Biophys. J.* 67: 1655–1668.